

Genetic correlations greatly increase mutational robustness and can both reduce and enhance evolvability

Sam F. Greenbury,¹ Steffen Schaper,^{2,3} Sebastian E. Ahnert,¹ and Ard A. Louis²

¹*Theory of Condensed Matter Group, Cavendish Laboratory, University of Cambridge, UK*

²*Rudolf Peierls Centre for Theoretical Physics, University of Oxford, UK*

³*Bayer Technology Services GmbH, BTS-TD-ET-CSM, Building B106, 51368 Leverkusen, Germany*

Mutational neighbourhoods in genotype-phenotype (GP) maps are widely believed to be more likely to share characteristics than expected from random chance. Such *genetic correlations* should, as John Maynard Smith famously pointed out, strongly influence evolutionary dynamics. We explore and quantify these intuitions by comparing three GP maps – a model for RNA secondary structure, the HP model for protein tertiary structure, and the Polyomino model for protein quaternary structure – to a simple random null model that maintains the number of genotypes mapping to each phenotype, but assigns genotypes randomly. The mutational neighbourhood of a genotype in these GP maps is much more likely to contain (mutationally neutral) genotypes mapping to the same phenotype than in the random null model. These *neutral correlations* can increase the robustness to mutations by orders of magnitude over that of the null model, raising robustness above the critical threshold for the formation of large neutral networks of mutationally connected genotypes that enhance the capacity for neutral exploration. We also study *non-neutral correlations*: Compared to the null model, i) If a particular (non-neutral) phenotype is found once in the 1-mutation neighbourhood of a genotype, then the chance of finding that phenotype multiple times in this neighbourhood is larger than expected; ii) If two genotypes are connected by a single neutral mutation, then their respective non-neutral 1-mutation neighbourhoods are more likely to be similar; iii) If a genotype maps to a folding or self-assembling phenotype, then its non-neutral neighbours are less likely to be a potentially deleterious non-folding or non-assembling phenotype. Non-neutral correlations of type i) and ii) reduce the rate at which new phenotypes can be found by neutral exploration, and so may diminish evolvability, while non-neutral correlations of type iii) may instead facilitate evolutionary exploration and so increase evolvability.

Keywords: genotype-phenotype map, neutral correlations, neutral networks, RNA secondary structure, protein quaternary structure, Polyomino, HP lattice model

I. INTRODUCTION

In a classic paper [1], published in 1970, John Maynard Smith introduced several key ideas for describing the structure of genotype-phenotype (GP) maps. He first outlined the concept of a protein space, the set of all possible sets of amino acid chains, and suggested that for evolution to smoothly proceed, these should be connected as networks of functional protein phenotypes that can be interconverted by (point) mutations. He then argued that one criterion for such networks to exist is for a protein X to have at least one mutationally accessible neighbour which is “meaningful, in the sense of being as good or better than X in some environment”. In other words, if X has N mutational neighbours, then the frequency f of “meaningful” proteins should satisfy $f > 1/N$. He pointed out that this was likely to be true in part due to the ubiquity of neutral mutations, which had been famously developed by Kimura [2] and King and Jukes [3] just a few years prior to his paper. But he also gave a second reason for expecting connected networks, namely that, “There is almost certainly a higher probability that a sequence will be meaningful if it is a neighbour of an existing functional protein than if it is selected at random.” This idea that mutational neighbours differ from the random expectation is what we will call *genetic correlations*.

Following Maynard Smith, many authors have explored the role of networks of genotypes connected by single point mutations. Lipman and Wilbur [4] first showed that large networks of mutationally connected genotypes mapping to the same phenotype are found in the Hydrophobic-Polar (HP) model for protein folding, introduced by Dill [5, 6]. They also pointed out that

neutral mutations allow a population to traverse these networks, facilitating access to a larger variety of alternate phenotypes. Schuster and colleagues [7] developed these themes further using detailed models for the secondary structure of RNA [8]. They coined the term “neutral network” to describe sets of mutationally connected genotypes that map to the same secondary structure phenotype. As RNA secondary structure is fairly easy to calculate and thermodynamics based models such as the Vienna package are thought to provide an accurate prediction of real RNA secondary structure [9, 10], the nature of neutral networks in these models has been extensively studied [7, 8, 11–16]. Since these pioneering works, neutral networks have been considered in GP maps of other biological processes, including models for gene networks [17, 18] metabolic networks [19] and the Polyomino model for self-assembling protein quaternary structure [20].

From these studies of model systems a number of basic principles have emerged, much of which has been admirably reviewed in important books by Wagner [15, 16]. Firstly, for neutral networks to exist, the GP map should exhibit *redundancy*, where multiple genotypes map onto the same phenotype. This many-to-one nature of the mappings is illustrated in Fig. 1. Redundancy is of course closely linked to the existence of neutral mutations [2, 3], although the relationship between these concepts is not entirely unambiguous. In the theory of neutral evolution, a mutation may lead to a slightly different phenotype, but as long as the change in fitness is small enough not to be visible to selection, it is considered to be effectively neutral [21]. Whether selection can act depends on the degree of phenotypic change, the environment, and other factors such as the population size and mutation rate. Therefore, identifying whether or not a mutation is neutral can be complex, and the answer may vary as parameters external to the GP map change with time. So while redundancy only couples identical phenotypes, and so is a more restrictive concept than neutral mutations, it has the advantage of sidestepping the subtle issues listed above and is

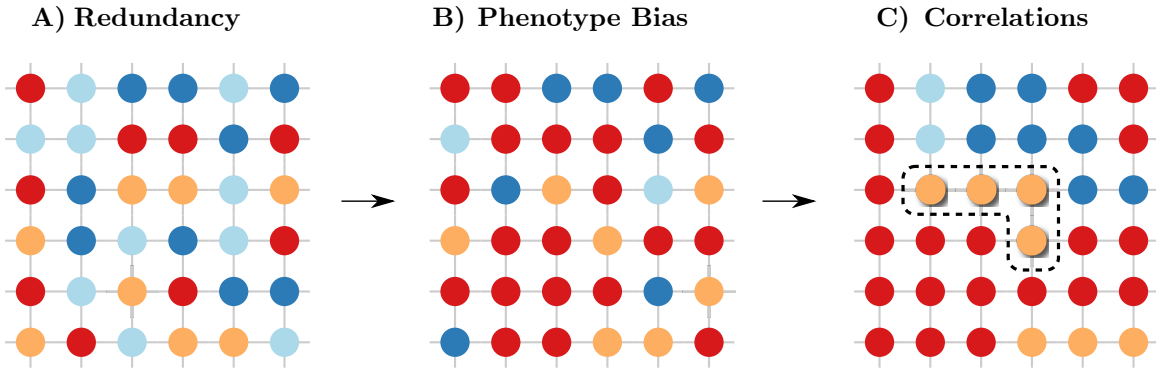


FIG. 1. **Schematic depiction of the GP map properties of redundancy, phenotype bias and neutral correlations.** Phenotypes are represented by colours, genotypes as nodes and mutations as edges. A) Each colour appears multiple times with uniform redundancy. B) Some colours appear more often than others, demonstrating a phenotype bias. C) A rearrangement of the colours from the middle plot illustrates neutral correlations. The black box surrounding the four orange genotypes depicts a single component (a set of genotypes connected by neutral point mutations, also called a neutral network) of the orange phenotype. Neutral correlations enhance the probability that such neutral networks occur.

more easily applicable to the study of a static GP map.

The second basic principle to emerge is that the number of genotypes per phenotype (the redundancy) can vary, leading to *phenotype bias*, as depicted in Fig. 1.

Thirdly, it is generally the case that the larger the redundancy, the greater the mean mutational robustness of genotypes mapping to that phenotype.

Fourthly, the larger the neutral network, the greater the variety of alternative phenotypes within one (non-neutral) point mutation of the whole neutral network, leading to robustness and measures of evolvability that count the number of different phenotypes that are potentially accessible being positively correlated [22].

Finally, a key principle, emphasised by Maynard Smith [1], but which has earlier roots in concepts such as the shifting balance theory off Sewall Wright [23], is that neutral mutations allow a population to access, over time, a wider variety of potential alternative phenotypes than would be available around a single genotype [4, 11, 16]. Evidence for the key role of these networks in promoting evolutionary innovation has been found, for example in experiments on RNA structures [24, 25] and transcription factors [26].

The main focus of this paper is genetic correlations. To explore and quantify how they affect concepts such as neutral networks, robustness and evolvability, we study genetic correlations in three of the GP maps mentioned above. These are the sequence to RNA secondary structure map and HP model for protein folding (tertiary structure), which have been extensively studied, as well as the more recently introduced Polyomino model for self-assembling protein quaternary structure. Several properties of these three GP maps have recently been compared [20, 27], but a detailed investigation of their genetic correlations has not yet been considered.

In order to quantify genetic correlations we must first define an uncorrelated null model to which the biophysical GP maps can be compared. We employ a random GP map that was recently introduced in ref. [14]. It shares the following properties with the biological GP map to which it is being compared: the same alphabet size K , genome length L , number of 1-mutation neighbours $(K-1)L$, number of genotypes $N_G = K^L$, number of phenotypes N_P , and frequencies f_p , defined as the fraction of all genotypes that possess phenotype p . We summarise the GP map nomenclature used in this paper in Table I.

Properties shared by random and biological GP maps	Symbol
<i>Alphabet size:</i>	K
<i>Genotype length:</i>	L
Number of 1-mutation neighbours of a genotype:	$(K-1)L$
Number of genotypes:	$N_G = K^L$
Number of phenotypes:	N_P
<i>Redundancy:</i> the size of neutral set or the number of genotypes that map to phenotype p	F_p
<i>Phenotype frequency:</i> the fraction of genotypes that map to phenotype p ,	$f_p = \frac{F_p}{N_G}$
Properties that differ between random and biological GP maps	Symbol
<i>Neutral set:</i> all genotypes that map to phenotype p	\mathcal{G}_p
<i>Neutral component:</i> A subset of \mathcal{G}_p that is fully connected by point mutations. Also called a <i>neutral network</i> .	NN
The number of 1-mutation neighbours of genotype g mapping to phenotype p	$n_{p,g}$
<i>Phenotype robustness:</i> mean robustness of all genotypes mapping to a phenotype p	ρ_p
<i>Phenotype mutation probability:</i> Probability that a point mutation from a genotype mapping to phenotype p will generate a genotype mapping to phenotype q	ϕ_{qp}

TABLE I. **GP map nomenclature.** GP map properties and their algebraic representations.

The only difference between a biophysical model and its associated null model is that the $F_p = f_p \times N_G$ genotypes for each phenotype p are each randomly assigned to the set of N_G possible genotypes. Of course one does not expect real genotype spaces to be randomly populated in this way but this expectation is what motivates the null model. Because the two GP maps share the same global properties, the comparison can help identify and quantify non-random features of how genotypes are organised across the genetic space, and so should shed light on nature of the correlations that Maynard Smith introduced.

The paper is organised as follows. We first examine *neutral correlations*, schematically illustrated in Fig. 1, through considering the relative likelihood that mutationally neighbouring genotypes possess the same phenotype in the biological GP map and its random counterpart. We then perform a similar analysis for *non-neutral correlations*. Since these different kinds of correlations all modulate the way that novel variation arises

through random mutations, we finish by commenting on how correlations affect subtle interplay of robustness and evolvability [15, 28], and also briefly suggest a few other forms of correlation that could be studied in GP maps.

II. METHODS

A. Random GP maps: a null model

As described in the introduction, the random GP map has the same alphabet size K , genotype length L , number of phenotypes N_P , number of genotypes $N_G = K^L$, and set of phenotype frequencies $\{f_p\}$ as its associated biological GP map, except that the genotypes are randomly assigned to the phenotypes in a way that maintains the set of frequencies $\{f_p\}$ (or redundancies $\{F_p\}$) taken from the associated biological GP map. Thus several key *global* properties are the same, but many *local* properties linked to the geometry of neighbouring genotypes, are expected to be different. In contrast to approaches based on network theory [13], our null model focuses on the randomisation of the GP map, rather than the neutral network topology, which leaves the underlying lattice topology of the genotype network intact.

B. Biological GP maps: RNA, Polyomino and HP models

We consider three separate GP maps for low-level self-assembling biological systems: a model for RNA secondary structure [8], the HP lattice model for protein tertiary structure [5, 6] and the Polyomino model for protein quaternary structures [20, 29, 30]. All three of these models have been previously compared in ref. [20], and below we briefly outline the three different systems.

1. Vienna package for RNA secondary structure

In the widely studied RNA secondary structure GP map [7, 8, 11–16], the genotypes are sequences made of an alphabet of four different nucleotides, and phenotypes are the secondary structures, which describe the bonding pattern in the folded structure with the lowest free energy for the given sequence. Here, we use the popular Vienna package [8], which uses an empirical free-energy model and dynamic programming techniques to efficiently find the lowest free energy structures. We use Version 1.8.5 with all parameters set to their default values. The RNA GP map for length L is referred to as RNAL. We present results from RNA12, with $4^{12} \approx 16.8 \times 10^6$ genotypes mapping to 57 folded phenotypes, RNA15 with $4^{15} = 1.07 \times 10^9$ genotypes mapping to 431 folded phenotypes and RNA20, with $4^{20} \approx 1.10 \times 10^9$ genotypes mapping to 11, 218 folded secondary structure phenotypes.

2. HP lattice model for protein tertiary structure

The HP lattice model represents proteins as a linear chain of either hydrophobic (H) or polar (P) amino acids on a lattice [5].

A simple interaction energy function is used between non-adjacent molecules in the chain. Hydrophobic-hydrophobic interactions are energetically favourable. We use an implementation with the interaction energy E between the different potential pairs being classified as $E_{HH} = -1$, with $E_{HP} = E_{PP} = 0$, as widely chosen by other authors, see e.g. [27, 31]. A phenotype is defined for each shape (fold) on the lattice that is the unique free energy minimum of at least one sequence. If a sequence has more than one structure as its minimum, then it is considered not to fold properly, and so is categorised as belonging to the (potentially deleterious) general non-folding phenotype. The compact HP model restricts the possible folds to those which are maximally compact, in an attempt to capture the globular nature of *in vivo* proteins [32]. We make use of both compact and non-compact HP GP maps by considering both the GP map for all folds of length, $L = 24$ (denoted HP24) and all compact folds on the 5×5 square grid (of length $L = 25$, denoted HP5x5). For the non-compact HP24 GP map there are $2^{24} \approx 16.8 \times 10^6$ genotypes and 61, 086 folded phenotypes, while for the compact HP5x5 model the $2^{25} \approx 33.6 \times 10^6$ genotypes map to a much smaller set of 549 unique folded phenotypes.

3. Polyomino model for protein quaternary structure

Protein quaternary structure describes the shape of a set of proteins that self-assemble into a well-defined cluster. The Polyomino GP map is a recently introduced lattice model which, in the spirit of the HP lattice model for tertiary structure, provides a simplified but tractable GP map for protein quaternary structure [20]. It employs a set of N_t square tiles with N_c interface types, together with a set of rules that denote how the interfaces bind. These sets are specified by genotypes in the form of linear strings.

If a given set of tiles self-assembles to a unique bounded shape (phenotype), the genotype is considered to map to that shape and represents a protein cluster. If on the other hand, the tile set does not always assemble to the same shape, or if it assembles to an unbounded shape (as occurs in sickle cell anaemia for example), then the genotype maps to the *undefined phenotype* (UND).

The GP map resulting from N_t kit tiles and N_c interface types is denoted as S_{N_t, N_c} . In this work, we consider $S_{2,8}$ which has 1.7×10^7 genotypes mapping to 13 different self-assembling phenotypes and the larger space $S_{3,8}$ which has 6.9×10^{10} genotypes mapping to 147 phenotypes.

4. A deleterious phenotype in all three GP maps

We also distinguish a *deleterious phenotype* (del) in all three GP maps. For the RNA GP map, this occurs when the unbonded strand is the free-energy minimum, so that the strand does not fold. For the HP model this occurs when a sequence does not have a unique ground state structure, which is interpreted as the protein not folding. For the Polyomino GP map this occurs when the set of tiles produces an UND structure. For RNA this del phenotype makes up 85% of RNA12, 65% of RNA15 and 33% of RNA20. In the HP model the fraction is typically larger, consisting of 98% of the HP24 map and 82% for the HP5x5 mapping, while for the Polyomino GP map we find 54%

of $S_{2,8}$ and 80% of $S_{3,8}$. For the RNA this fraction decreases with increasing genotype length L , while the converse is true for the Polyomino GP map and in the HP model the trend remains ambiguous [33].

III. RESULTS

A. Neutral correlations increase mutational robustness

In this section, we investigate robustness to point mutations and the close relationship between robustness and neutral correlations. The 1-robustness of a single genotype is straightforwardly defined as the number of genotypes that map to the same phenotype that are accessible within one point mutation. We also define three measures of mutational robustness that apply to whole phenotypes. Firstly, the *phenotype robustness* ρ_p of a phenotype p is defined as the fraction of 1-mutation neighbours to a given genotype that possess the same phenotype, averaged over the entire the neutral set \mathcal{G}_p [22]. This can be expressed algebraically as

$$\rho_p = \frac{1}{F_p} \sum_{g \in \mathcal{G}_p} \frac{n_{p,g}}{(K-1)L} \quad (1)$$

where $n_{p,g}$ is the number of 1-mutation neighbours of g with phenotype p .

The second quantity, which we call *generalised robustness* or *n-robustness* $\rho_p^{(n)}$, measures the phenotype robustness for a greater number of mutations. It is defined as the robustness of a genotype with phenotype p to n independent mutations to its genotype, rather than just the single mutation discussed above. This can be expressed algebraically as

$$\rho_p^{(n)} = \frac{1}{F_p} \sum_{g \in \mathcal{G}_p} n_{p,g}^{(n)} \frac{1}{\binom{L}{n} (K-1)^n} \quad (2)$$

where $n_{p,g}^{(n)}$ is the number of n -mutant neighbours of g with phenotype p and the normalisation on the right-hand of the sum is the total number of n -mutants. In the same way as for the phenotype robustness, the n -robustness is averaged across the neutral set \mathcal{G}_p of all genotypes that map to phenotype p .

The third quantity we introduce is the *average n-robustness* $\langle \rho^{(n)} \rangle$ which is the average of the n -robustness over all phenotypes in a given GP map:

$$\langle \rho^{(n)} \rangle = \frac{1}{N_P} \sum_{j \in \mathcal{P}} \rho_j^{(n)} \quad (3)$$

where \mathcal{P} is the set of all N_P phenotypes in the GP map. In contrast to the two previous definitions that measure robustness for a single phenotype, it is a general property of the whole GP map. One could imagine generalising this further to a subset of the phenotypes, for example those whose frequencies f_p are greater than the average N_P/N_G .

In the random model there are no correlations, so the probability that a genotype leads to phenotype p is given by its frequency f_p , independently of the identity of its neighbours. The phenotypic robustness therefore is simply

$$\rho_p = f_p$$

and the mean number of neutral neighbours is

$$\langle n_{g,p} \rangle = (K-1)Lf_p$$

which is the expectation value for a binomial distribution with $(K-1)L$ trials and probability of a given neighbour being f_p . It is independent of the identity of the genotype g . Similarly, since the probability of finding a phenotype is uniformly distributed over the genotype space, the n -robustness is given by

$$\rho_p^{(n)} = f_p$$

with the n -robustness is the same for all n , leading to an average n -robustness:

$$\begin{aligned} \langle \rho^{(n)} \rangle &= \frac{1}{N_P} \sum_{j \in \mathcal{P}} f_j \\ &= \frac{1}{N_P} \end{aligned} \quad (4)$$

since the phenotype frequencies in a GP map sum to unity.

These measures for robustness cannot be so easily derived analytically for the biological GP maps. Instead we calculate these properties from samples of genotypes for each phenotype in the GP maps, and compare them to the analytic results above for the random GP map.

In Fig. 2A, we compare the phenotype robustness of phenotypes across our three biological GP map models (see Methods for a detailed description) to the robustness of the associated random GP map. All the random models follow $\rho_p = f_p$ very closely, as expected (we only show one schematic random map in the figure, but the others have the same behaviour). By contrast, the three biological GP maps have a much larger robustness. Very roughly, we find that $\rho_p \propto \log f_p$, so that the relative difference between the biophysical models and the associated random model grows rapidly with decreasing frequency f_p , and can easily reach several orders of magnitude. What this tells us is that the biological genetic spaces are correlated – the probability that a neighbour maps to the same phenotype is much larger than the uncorrelated prediction from random chance.

We next consider the average n -robustness against the radius n for the three GP maps $S_{2,8}$, RNA12 and HP24. A sample of 100 genotypes for each phenotype in the respective systems is taken (apart from HP24 where a sample of 100 randomly chosen phenotypes is made due to the large number of phenotypes) and the n -robustness is measured and averaged over phenotypes. In Fig. 2B, we plot the average n -robustness at each radius along with the flat expectation lines from Eq. 4 for the random versions of the biological GP maps. In all three cases we observe a decay from greater than the null values for small radii to slightly less than the null expectation at larger radii. This is another indication that the proximal genotypes are more likely to be of the same phenotype (neutrally correlated) and, therefore, a greater robustness is found locally. At larger distances, the robustness decreases below the null level because there are a greater number of genotypes at closer distances and the total frequency must balance to the average that is the null expectation line.

We can also define a *neutral correlation length* from the decay of the average n -robustness with n , for example as the distance where $\rho_p^{(n)}$ first crosses the random-null expectation. Clearly this length is zero for the random model, which has no correlations. Very roughly, this procedure gives a correlation length of $n \approx 7$ for the RNA model, $n \approx 5$ for the Polyomino

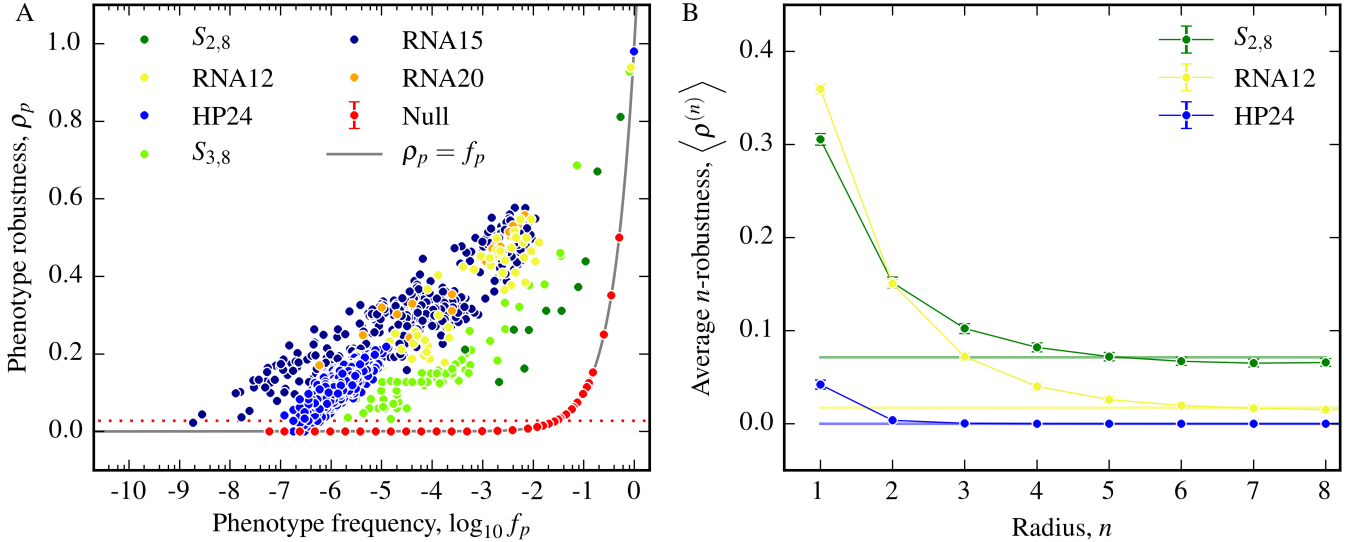


FIG. 2. **Neutral correlations lead to larger mutational robustness** A) The phenotype robustness ρ_p is plotted as a function of frequency f_p for all phenotypes in the RNA secondary structure models: RNA12, RNA 15, RNA20, the Polyomino models for protein quaternary structure: $S_{2,8}$, $S_{3,8}$ and the HP protein folding model HP24. Each model has an associated random model with the same frequencies, but we only show one example, with $K = 4$ and $L = 12$ and a set of phenotypes chosen with a broad range of frequencies to best illustrate the relationship (red points). All random models closely follow the expected theoretical curve $\rho_p = f_p$ (grey line). The biophysical models exhibit a much larger robustness than the random models, which is a mark of neutral correlations. The red dotted line is $1/\delta$ (Eq. (5)) for $K = 4$, $L = 12$. If $(\rho > 1/\delta)$ then large neutral networks are expected, which is much more likely for the biophysical models than for the random model. B) The average n -robustness $\langle \rho^{(n)} \rangle$, defined in Eq. 3, for each of the three biological GP maps, along with the expected values $\langle \rho^{(n)} \rangle = 1/N_P$ for the associated random null models (flat coloured horizontal lines) is plotted against n . Across all three GP maps, we see a typical decay in robustness towards the random null model expectation with increasing mutational distance. From this decay a neutral correlation length can be defined which is shorter for the HP model than for the other two models. Error bars are the standard error on the mean of the average n -robustness, which was sampled.

model while for the HP model it is noticeably shorter at $n \approx 2$. All three models are for fairly small genome length L , so one should be careful of reading too much into the numerical values of these correlation lengths. However, it may very well be that this ordering of models will persist for larger L .

B. Neutral correlations produce larger and fewer components

Having shown that the biophysical models have much larger robustness than the random model, and therefore exhibit neutral correlations, we next investigate how this increased probability for neutral neighbours affects the way genotypes are connected into networks.

The neutral set \mathcal{G}_p is the set of all genotypes mapping to phenotype p . A component is the subset of the neutral set \mathcal{G}_p that is connected by single point mutations. We use this term because it is commonly used in graph theory to denote a set that is connected. Although the literature can be somewhat ambiguous, with the term neutral networks sometimes referring to the neutral set, and sometimes to a neutral component, we take a neutral network to be synonymous to a neutral component in this paper because if we have only point mutations then a population can only explore a neutral component and may not be able access the whole neutral set.

There are several reasons why a neutral set may not be fully connected by neutral point mutations. If the genotypes are too diffusely spread out over the full genotype space, then they may be disconnected. But in some cases basic biophysical con-

straints also lead to fragmentation. For example, in RNA, a CG bond in a stem motif cannot be turned into a GC bond without breaking the bond [34], a form of neutral reciprocal sign epistasis [35]. For a secondary structure stem motif of n bonds, this phenomenon breaks the neutral set up into at least 2^n separate components, often of similar size, that are connected by point mutations internally, but which need at least two mutations to be connected together.

We begin by comparing the size of neutral components in the random null model to those found in our biological GP maps. In the random model, there are two important threshold values: firstly, the *giant component onset*, when a phenotype's components change from being largely isolated to forming larger connected clusters, and secondly, the *single component onset* where virtually all genotypes are taken up by a single giant connected component.

As each genotype has many neighbours, a simple mean-field-like approach from *percolation theory* for random graphs [36] should be fairly accurate. This suggests that the giant component onset begins when the average number of neighbours of a given genotype with the same phenotype is approximately unity, which was also the criterion used by John Maynard Smith [1]. For the null model, where phenotypes are assigned to genotypes completely randomly, this reduces to an explicit threshold frequency

$$\delta = \frac{1}{(K-1)L} \quad (5)$$

such that we expect the giant components for phenotypes with $f_p \gtrsim \delta$. It can be shown analytically in the limit $L \rightarrow \infty$ [34]

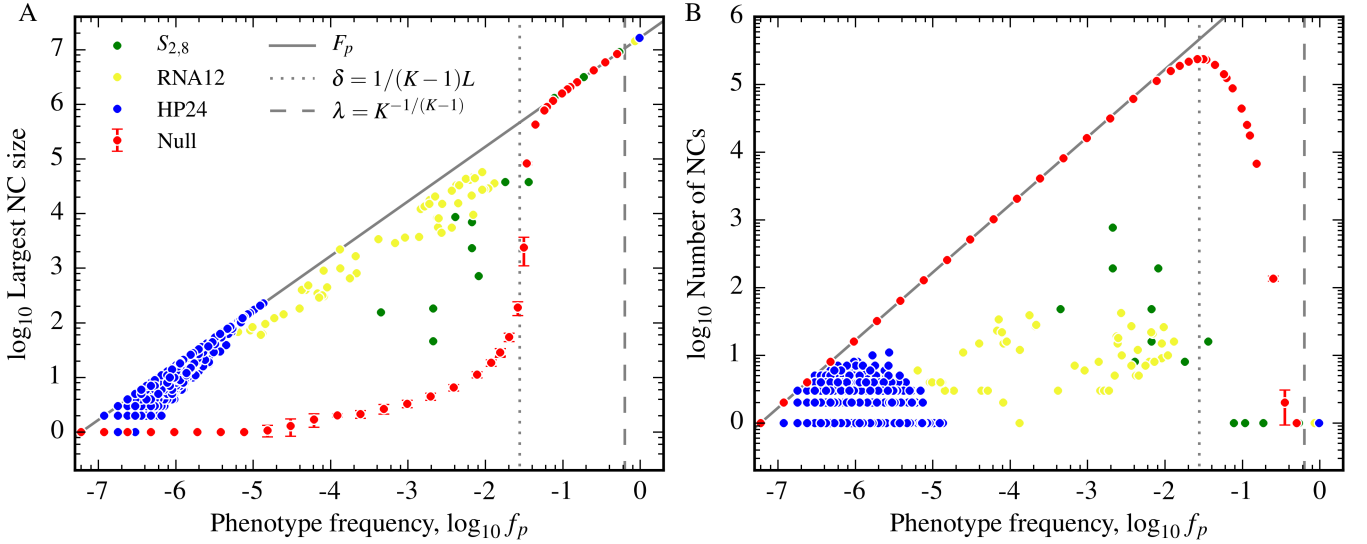


FIG. 3. **Biological GP maps have much larger and fewer neutral components than their random counterparts due to neutral correlations.** A) The logarithm of the largest neutral component for a given phenotype is plotted as a function of frequency for random null models (with $K = 4$, $L = 12$) and three biological GP maps, RNA12, $S_{2,8}$ and HP24. The vertical dotted line denotes the giant competent threshold $\delta \approx 1/36$, defined in Eq. (5), for the schematic random model with $K = 4$, $L = 12$. The vertical dashed line denotes the single component threshold $\lambda \approx 0.37$, defined in Eq. (6), for the schematic random model. The biological GP maps show much larger connected components below these thresholds, due to the presence of neutral correlations. B) The logarithm of the total number of neutral components against frequency is plotted for the same models. The theoretical thresholds δ and λ work well for random model but again the number of components in the biophysical models differ greatly from the random model expectation due to the presence of correlations. In both plots, error bars represent a single standard deviation from the 100 independent realisations of the random null model used to derive the neutral component statistics.

that there is another transition at

$$\lambda = 1 - \frac{1}{K^{\frac{1}{K-1}}} \quad (6)$$

where, for $f_p \gtrsim \lambda$, all the components coalesce into one single giant component, so that the neutral set should be (nearly) fully connected. While the giant component threshold δ scales as $1/L$, so that it decreases for larger maps, the single component threshold λ from Eq. 6 is independent of genome length L , and only varies with alphabet size. For example, $\lambda = 0.5$ for $K = 2$ and $\lambda \approx 0.37$ for $K = 4$. These are large frequencies that are unlikely to be reached for more than a single phenotype in any realistic GP maps.

In Fig. 3, we plot how the largest component size (left) and number of components (right) varies with frequency in both a null model ($K = 4$, $L = 12$) and three GP maps $S_{2,8}$, RNA12 and HP24. We first focus on the simple schematic null model. Data is calculated by averaging over 100 independent realisations of the random mapping of genotypes to phenotypes in a way that preserves the frequencies. The largest component size and the number of components formed by the phenotype are then measured. These values are shown in Fig. 3 for an array of frequencies in the schematic null GP map. Below the giant component onset $\delta \approx 1/36$, most genotypes are completely isolated – the total number of neutral components scales with f_p . Around the giant component threshold δ , this scaling changes markedly, and instead the size of the largest neutral components scales linearly with f_p and takes up the majority of the genotypes in the neutral set. The number of components continues to decline until f_p exceeds the giant component connectivity threshold $\lambda \approx 0.37$, at which point there is just one component and the neutral set is completely connected.

We next consider the biological GP maps relative to the behaviour exhibited by the null model. Firstly, all three GP maps have much larger maximum neutral set sizes than the random model. This is not surprising, as Fig. 2A shows that, due to neutral correlations, $\rho_p > \delta$ for most phenotypes in each system ($\rho = 1/\delta$ for $K = 4$, $L = 12$ is shown as a dotted red line in the plot). Once the probability of having a neutral neighbour is above the δ threshold, we expect large networks. For HP24 and RNA12, the largest neutral component size clearly grows linearly with frequency, and so scales linearly with the size of the neutral set. For the Polyomino space $S_{2,8}$ this scaling is less evident, but the components are still much larger than their random counterparts would be.

Secondly, for all three models, the number of components does not vary much with f_p , in contrast to the random model where this number scales, as expected, with the neutral set size if $f_p \lesssim \delta$. Since these components typically have robustness above δ or even λ , the reason there are still multiple components must be due to biophysical constraints which are not present in the random model, such as the non-reciprocal sign epistasis discussed earlier for RNA. These effects are to first order independent of f_p which explains why the number of components does not correlate with f_p . In each of these three models the largest “phenotype” of all is the deleterious non-folding or non-assembling one. Its frequency exceeds the threshold λ and its neutral set is fully connected.

We conclude that the biophysical models considered here have large neutral networks even for frequencies f_p that are several orders of magnitude lower than the random model large component threshold δ . The abject failure of the random model to predict the robustness and the neutral network size highlights the importance of neutral correlations in these systems.

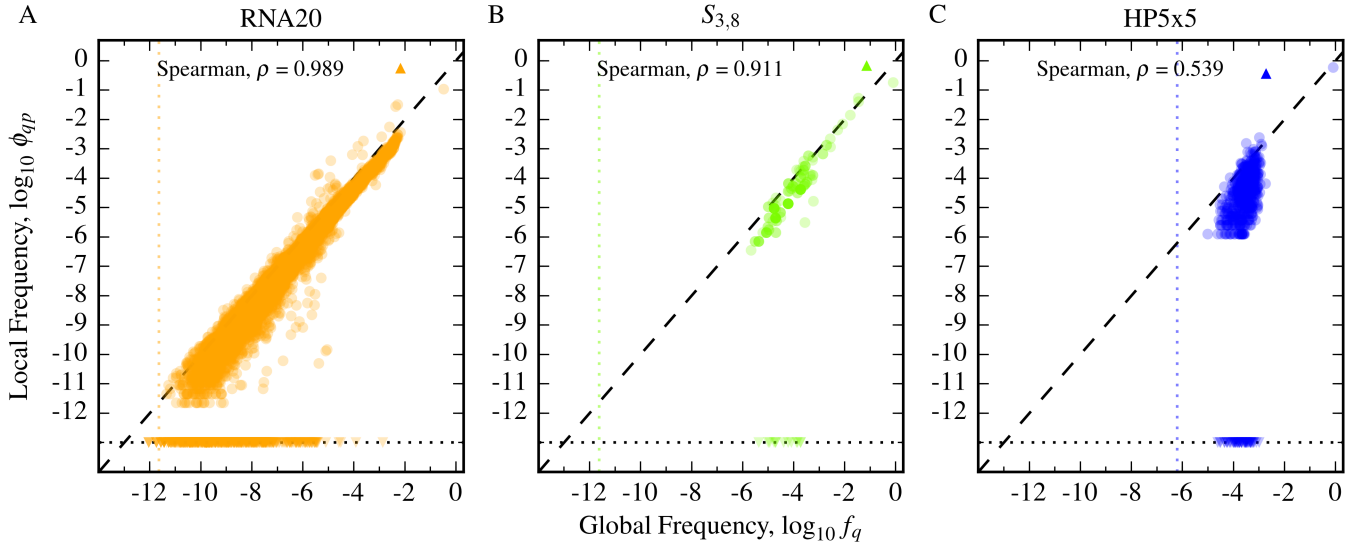


FIG. 4. **Phenotype mutation probabilities scale with global frequency.** We plot the relationship between ϕ_{qp} (circles) and f_q for the largest non-deleterious phenotype p in $S_{3,8}$ and HP5x5, and for the second largest in RNA20 (not the largest due to computational expense). We see in each case a strong positive correlation (p -value $\ll 0.05$ in all cases), very similar to the expectation for the null model (not shown here, but for which the correlation is exact to within statistical fluctuations, see ref. [14] and Appendix A). Spearman rank correlation coefficients are shown in the top-left of each plot. Differences from $\phi_{qp} = f_q$ are relatively small compared to the overall range of variation, except for sets of phenotypes that are not connected at all, which typically arise due to biophysical constraints. These are shown as downward triangles along the lower horizontal dotted line which represents $\phi_{qp} = 0$. For each plot, the upward triangle indicates $\phi_{pp} = \rho_p$, the phenotype robustness, which is always over-represented ($\rho_p > f_p$) due to neutral correlations.

C. Non-neutral phenotype mutation probability

We next consider non-neutral mutations. The first question is: Are two different phenotypes, on average, more or less likely to be connected to each other than one would expect by chance? To address this question, we employ a generalisation of robustness, namely the *phenotype mutation probability* ϕ_{qp} of q with respect to p , defined as the fraction of 1-point mutations of genotypes in the neutral set for phenotype p that map to phenotype q . This can be written as:

$$\phi_{qp} = \frac{1}{F_p(K-1)L} \sum_{g \in \mathcal{G}_p} n_{q,g}.$$

Thus ϕ_{qp} averages a local property, $n_{q,g}$ – the number of genotypes that map to phenotype q found the 1-mutation neighbourhood of a genotype that maps to phenotype p – over the entire neutral set \mathcal{G}_p . Note that this phenotype mutation probability is not symmetric ($\phi_{qp} \neq \phi_{pq}$) and that, if $p = q$, it reduces to the phenotype robustness $\phi_{pp} = \rho_p$. It has recently been shown [14] that ϕ_{qp} is a key quantity for incorporating the structure of a GP map into population genetic calculations. In the null model we expect $\phi_{qp} = f_q$ to be an excellent approximation [14], with the caveat that it must be possible for enough genotypes to be sampled. What do we mean by enough genotypes? Given a phenotype p with redundancy F_p , there are at most $F_p(K-1)L$ unique neighbours available. This number provides an upper bound – in reality, several neighbours of one genotype will also be neighbours of another genotype with the same phenotype, resulting in a reduction in the number of unique neighbours. However, this allows us to define a mini-

num threshold

$$\gamma = \frac{1}{F_p(K-1)L} \quad (7)$$

If $f_q \lesssim \gamma$, then the probability that a phenotype p has a genotype leading to phenotype q is less than one, and the probability that $\phi_{qp} = 0$ due to statistical fluctuations becomes appreciable. Further detail on how ϕ_{qp} and F_p relate when the threshold is not satisfied, which is mainly relevant for smaller GP maps and for lower F_p , is provided in Appendix A. Here we focus on phenotypes with larger F_p , in the larger GP maps of the previous section that do effectively sample the space of phenotypes.

In Fig. 4, we plot the relationship between the phenotype mutation probability ϕ_{qp} and global frequency f_q around the RNA20 phenotype with the second largest neutral set, the assembling phenotype for $S_{3,8}$ with the largest neutral set, and the HP5x5 folding phenotype with the largest neutral set. For phenotypes in $S_{3,8}$ and HP5x5, with such large numbers of genotypes, every phenotype q will be effectively sampled, as all phenotypes have f_q values that are significantly above $f_q = \gamma$ (vertical dotted lines), which is the approximate threshold at which at least one genotype of phenotype q would be expected to be found. A small fraction of phenotypes lie close to the $f_q = \gamma$ threshold for RNA20, but by far the majority may be expected to be effectively sampled. For RNA20 and $S_{3,8}$, we observe a very strong and highly significant positive correlation with the random null model expectation $\phi_{qp} = f_q$. In HP5x5, there is also a strong positive correlation, though less strong than in the RNA and Polyomino cases, with a greater number of phenotypes falling below the one-to-one expectation. We did not plot the non-compact model HP24 because most of its frequencies are below the threshold γ (see Appendix A).

To summarise, in contrast to the robustness $\rho_p = \phi_{pp}$ where

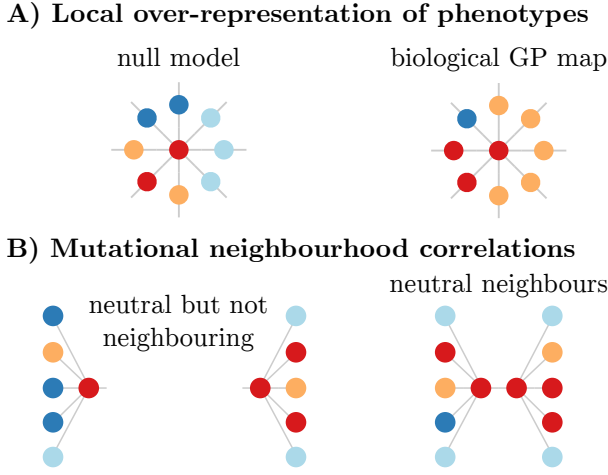


FIG. 5. **Illustration of further non-neutral correlations.** A) On the right, the orange phenotype is over-represented relative to the null model: The red genotype in the centre has more orange neighbours than would be expected by the global frequency of orange. B) The phenotypes that appear in the mutational neighbourhood of two neutral neighbours are expected to be more similar (right) than two non-neighbouring genotypes of the same phenotype (left).

neutral mutations lead to strong deviations from the null model, the non-neutral phenotype mutation probabilities follow the random model expectation that $\phi_{qp} \approx f_q$ remarkably well. There are still important deviations, especially for those phenotypes that can not be reached due to biophysical constraints so that $\phi_{qp} = 0$ [35]. Moreover, it may be an interesting exercise to look more closely at phenotypes for which ϕ_{qp} is significantly greater or less than f_q as such deviations could signal similarities or differences between phenotypes. For example, two RNA phenotypes with similar hairpin topology, but perhaps a difference of one bond in a stem may have a larger probability of interconverting than topologically more dissimilar RNA phenotypes. The difference between ϕ_{qp} and f_q could then be used to quantify the difference between phenotypes p and q . These more subtle types of correlation are beyond the scope of this paper. At any rate, compared to the result in the previous sections showing the strength of neutral correlations, the dominant agreement with the random model is apparent. However, given that ϕ_{qp} is averaged over a neutral set, it may be that there are *local* non-neutral correlations that are obscured by the averaging. With this in mind, we next investigate such local correlations.

D. Non-neutral local over-representation correlations

We first describe *non-neutral local over-representation correlations* which mean that, given phenotype q is found in the 1-mutation neighbourhood of a genotype g (which maps to phenotype $p \neq q$), then phenotype q will appear a greater number of times in total than predicted by f_q or ϕ_{qp} in this 1-mutation neighbourhood, as pointed out in ref. [22]. These correlations are illustrated in Fig. 5A.

To measure 1-mutation neighbourhoods, we sample randomly chosen genotypes g from the neutral set \mathcal{G}_p , with a genotype of phenotype q in its neighbourhood. We then measure the phenotype of all other neighbours of g . From this sample, we obtain the probability $P(q, p, m)$ of q occurring m times in the

1-mutation neighbourhood of a genotype mapping to phenotype p , given that q occurs at least once.

Two control null expectations may also be derived for $P(q, p, m)$. In the random model where phenotypes are randomly assigned, given q is in the 1-mutation neighbourhood of a genotype g (at a specific genotype g'), the probability may be calculated as a binomial probability based upon the overall frequency of q , leading to

$$P_1(q, p, m) = \binom{L(K-1)-1}{m-1} f_q^{m-1} (1-f_q)^{L(K-1)-m} \quad (8)$$

A second null expectation calculates the binomial probability by replacing f_q in Eq. 8 above by using the phenotype mutation probability ϕ_{qp} for the GP map instead:

$$P_2(q, p, m) = \binom{L(K-1)-1}{m-1} \phi_{qp}^{m-1} (1-\phi_{qp})^{L(K-1)-m} \quad (9)$$

In contrast to $P_1(q, p, m)$, this form accounts for any overall phenotypic heterogeneity known to be present in the GP map.

We compare the actual local prevalence against these two null expectations in Fig. 6. For RNA20, $S_{3,8}$ and HP5x5 we chose the same three phenotypes for phenotype q as we did in the previous section, while for phenotype p we choose one-by-one the next $n = 10$ largest (non-deleterious) phenotypes available in the GP map. By sampling 10,000 neighbourhoods for each of the $n = 10$ phenotypes for p , we calculate an average for $P(q, p, m)$ across the phenotypes ($\bar{P}(q, p, m)$) and compare this in Fig. 6 to the averages for the null expectations $\bar{P}_1(q, p, m)$ and $\bar{P}_2(q, p, m)$. For each biological GP map, q is more likely to be over-represented, that is to appear multiple times if it appears at least once when compared to the null expectations, leading to a skewed distribution compared to the control case. The most striking result is seen in RNA20, where there is a substantial tail to the distribution. We use average measures here to provide the general profile, smoothing out particular features that may occur between individual pairs of phenotypes q and p , but the local over-representation is seen for any of the phenotype pairs considered.

One consequence of these local over-representation correlations is that the probability that a genotype p has q *at least once* is less than expected from ϕ_{qp} , because those genotypes that have p multiple times take up more than the average share of the possible connections. For example, in the RNA20 GP map, with the most frequent of the set of phenotypes used for p and the next most frequent used as q , the probability of finding q at least once is 0.12 versus a null expectation of $1 - (1 - \phi_{qp})^{(K-1)L} = 0.20$. Thus these correlations lead to heterogeneity in the connections between phenotypes.

How these correlations affect evolutionary dynamics will depend on the regime being explored [14]. If the population is neutrally exploring genotypes that map to phenotype p , then in the monomorphic regime of evolutionary dynamics, where $NL\mu \ll 1$, this heterogeneity will lead to a significant drop in the rate at which q is first discovered by neutral exploration. In the polymorphic regime where $NL\mu \gg 1$, and different individuals in the population have different genotypes, the rate at which novel variation with phenotype q occurs may not be that different from the expectation given by ϕ_{qp} , at least if the population is spread across a large enough number of different genotypes to average over local heterogeneity.

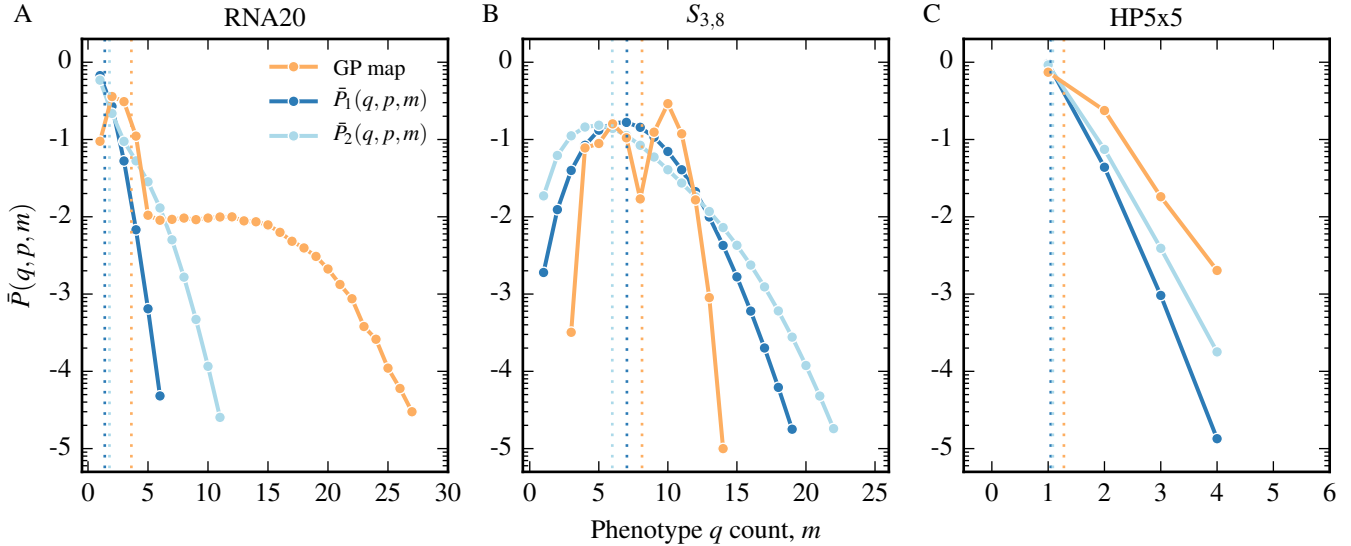


FIG. 6. **Non-neutral local over-representation correlations result in phenotypes being more likely to be found multiple times around genotypes.** We pick the same frequent phenotypes q in each of our biological GP maps as used in Fig. 4, and consider the prevalence of q around genotype g with phenotype p , given that q occurs at least once in the 1-mutation neighbourhood of g . The average of $\bar{P}(q, p, m)$ across the $n = 10$ most frequent phenotypes p in the neighbourhood of q (with $p \neq q$ and $p \neq \text{del}$), is compared to the respective averages for random null expectations $\bar{P}_1(q, p, m)$ and $\bar{P}_2(q, p, m)$ defined in the text. The mean of each distribution is plotted as a dotted line in each case. Contiguous sections with a probability greater than 10^{-5} are joined with lines in order to guide the eye. The mean value of m for each of the biological GP maps and the two random controls are shown as respective dotted lines with the same colours. Compared to the two null expectations of occurrence, q is over-represented locally as demonstrated by the shift of the means to the right.

E. Non-neutral local mutational neighbourhood correlations

We next examine *non-neutral local mutational neighbourhood correlations* which are illustrated schematically in Fig. 5B. They show that the 1-mutation neighbourhoods of two genotypes connected by a neutral point mutation are more likely to have similar phenotypic compositions than would be expected by two randomly chosen neutral non-neighbouring genotypes of the same phenotype. This type of correlation has already been demonstrated to exist for RNA [37]. To measure the similarity of neighbouring genotypes' mutational neighbourhoods, we consider the local quantity $\phi_{q,g}^{(\text{local})} = n_{q,g}/(K-1)L$, which becomes ϕ_{qp} when averaged over the whole neutral set \mathcal{G}_p . We compare the $\phi_{q,g}^{(\text{local})}$ for neighbouring genotypes with non-neighbouring genotypes in both the null model and biological GP maps. The similarity or difference could be measured in several different ways. The statistical measure we employ here is the Bhattacharyya coefficient [38], which for two discrete probability distributions x_i and y_i may be expressed as

$$BC(x_i, y_i) = \sum_i \sqrt{x_i y_i} \quad (10)$$

varying between 0 and 1 for maximally dissimilar and identical discrete probability distributions respectively.

To quantify whether neutral neighbours g and h have more similar phenotype distributions in comparison to non-neighbouring neutral genotype pairs g and g_2 , we compared the *similarity ratio* of the Bhattacharyya coefficients, $BC(g, h)/BC(g, g_2)$, using the $\phi_{q,g}^{(\text{local})}$ to define the distributions. A ratio greater than unity indicates that the phenotype distributions around neutral neighbours are more similar than the randomly selected neutral pair, and vice versa. We remove

the $K - 2$ mutual neighbours of g and h from the distributions as these will automatically contribute to similarity between the neighbourhoods in a trivial manner which we wish to exclude.

In Fig. 7 we plot histograms of the similarity ratio for 10,000 samples of g , h and g_2 in RNA20, $S_{3,8}$ and HP5x5, where the chosen phenotype is the same p as in the previous subsection. For 10,000 samples the means are 1.357 ± 0.003 for RNA20, 1.063 ± 0.001 for $S_{3,8}$ and 1.025 ± 0.001 for HP5x5, where the error is the standard error on the mean. For RNA20 and $S_{3,8}$, a clear skew in the overall distribution may be visually observed, demonstrating that neutral neighbours, on average, have more similar mutational neighbourhoods. HP5x5 also has the mean of its distribution at a value slightly larger than unity but it is much more marginal in this case, and the skew is harder to detect. We note that in general, the non-neutral correlations are weakest for the HP5x5 model. Finally, just as is the case for the non-neutral local over-representation correlations of the previous section, these local mutational neighbourhood correlations also reduce the rate at which novel phenotypes would be discovered by neutral exploration since a neutral neighbour is more likely to have some of the same phenotypes in its mutational neighbourhood, and so fewer alternatives.

F. Non-neutral deleterious phenotype correlations

The final, and perhaps most important, type of non-neutral correlation we consider is the accessibility of the deleterious phenotype from folding or self-assembling phenotypes, which we call *non-neutral deleterious phenotype correlations*. This type of non-neutral correlation is closest to the type of correlation suggested by Maynard Smith [1].

In Fig. 8 we plot histograms of the ratio $\phi_{\text{del},p}/f_{\text{del}}$ for all

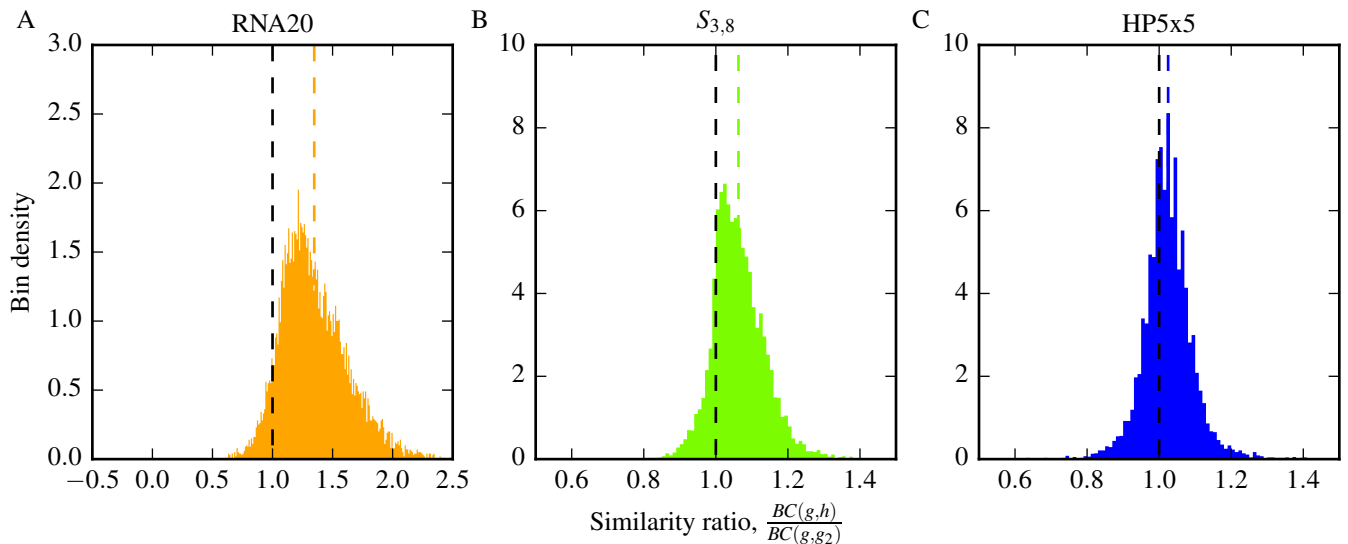


FIG. 7. **Non-neutral local mutational neighbourhood correlations result in mutational neighbourhoods of neutral neighbours being more similar than randomly selected neutral pairs.** Using the ratio of Bhattacharyya coefficients defined in Eq. (10), we show that neutral neighbours (g and h) have a closer phenotype probability distribution than a randomly chosen neutral pair (g and g_2). This is seen through the ratio being skewed with a mean (coloured vertical dashed lines) larger than unity (black vertical dashed lines). The standard error on this mean is negligible compared to the distance of the mean from one.

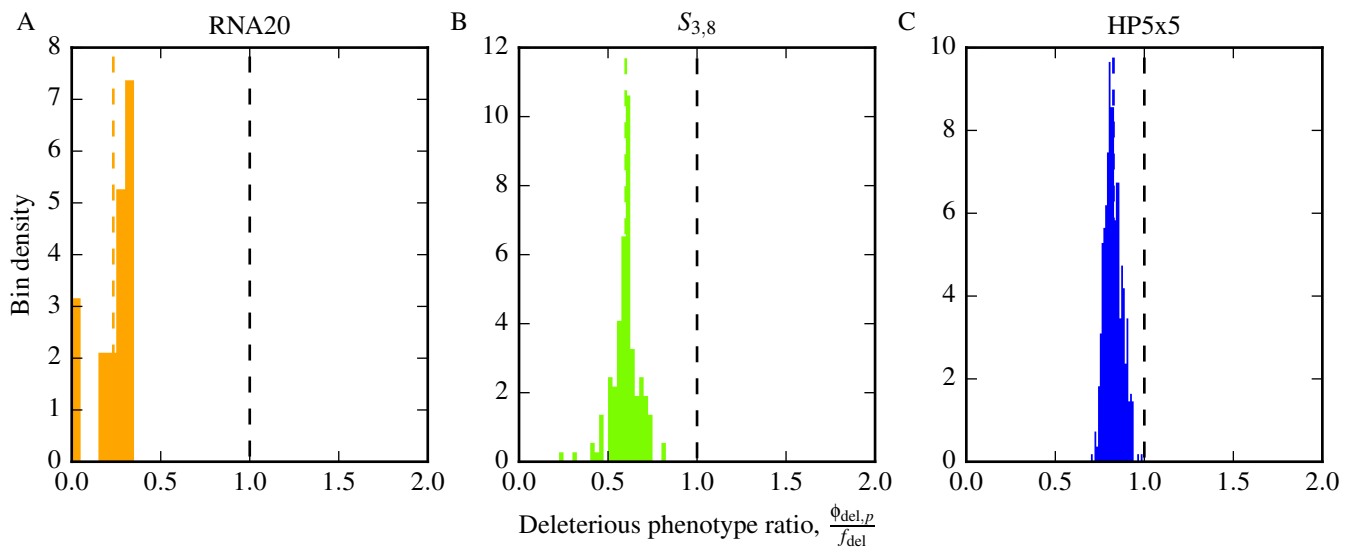


FIG. 8. **Non-neutral deleterious phenotype correlations: The deleterious phenotype is under-represented in the neighbourhood of folding or self-assembling phenotypes.** Histograms of the ratio of the phenotype mutation probability ($\phi_{\text{del},p}$) divided by the null model expectation of the global frequency (f_{del}) for the deleterious phenotype (non-folding for RNA/HP, non-assembling for Polyominoes). The distribution is clearly skewed to values < 1 , as highlighted by the dashed vertical coloured lines representing the mean in each case.

phenotypes p in $S_{3,8}$ and HP5x5, and the top 20 most frequent (largest f_p) in RNA20 (limited due to computational expense of this larger system). In all cases, we see that the deleterious phenotype is significantly less frequent around the non-deleterious phenotypes, due to the corresponding over-representation of the deleterious phenotype around itself. As a corollary of this effect, we also find $\rho_{\text{del}}/f_{\text{del}}$ equal to 1.10, 1.16 and 1.19 for RNA12, $S_{3,8}$ and HP5x5 respectively, illustrating a corresponding local over-representation of the deleterious phenotype in its own mutational neighbourhoods.

IV. DISCUSSION AND CONCLUSIONS

In this paper, we have explored the role of genetic correlations, which we defined and quantified as the difference in how genotypes are mutationally connected for biologically relevant GP maps, compared to a random null model with the same global properties (alphabet size, genome length, and number of genotypes per phenotype). Genetic correlations provide a simple conceptual framework within which a number of topological properties of GP maps can naturally be captured.

Firstly, *neutral correlations* mean that phenotypic robustness can be orders of magnitude larger than one would expect by random chance. This enhanced probability of encountering a genotype mapping to the same phenotype can extend to multiple mutations away from genotypes, which can be further quantified with a neutral correlation length. The correlation length is larger in the RNA secondary structure model and the polyomino model of protein quaternary structure than it is in the HP model for protein tertiary structure.

The role of mutational robustness in evolutionary dynamics has been much discussed [15, 16, 39–41] and an open question is whether and how such robustness has been selected for by natural selection [39]. Here we show that phenotypes are on average already much more robust than one would expect from random chance. At this level of analysis, the enhanced robustness is not caused by selection, but rather arises because the internal constraints of a GP map – the way that genotypes map to phenotypes – naturally lead to neutral correlations. It may still be the case that more robust genotypes can be selected for within a neutral set, or that these genotypes are favoured in certain dynamic regimes [40]. It may also be true that in some cases a particular phenotype is preferred by selection because it is more robust than an alternative one. But even if this is so, in this case natural selection is still acting on variation that is already naturally quite robust due to neutral correlations.

In an important study of experimentally measured binding affinities for transcription factors, Payne and Wagner [26] showed that the mutational robustness of a phenotype correlates positively with its evolvability, measured as the number of alternate phenotypes in the 1-mutation neighbourhood of the neutral set. Interestingly, their measured robustnesses are significantly larger than the global frequencies, which suggests neutral correlations similar to those observed in the models we study in the current paper. It would be interesting to see whether they could also measure a neutral correlation length in this system, as well as the presence of significant non-neutral correlations.

The relationship between robustness and evolvability has been the subject of much discussion in the literature [12, 22, 41, 42]. Here we show, as already anticipated by Maynard Smith [1], that if the phenotype robustness is roughly larger than $\delta = 1/(K - 1)L$, so that the expected number of neutral neighbours is greater than one, then the phenotype will exhibit large neutral networks. Such networks may be critical for the capacity to access novelty. In the random model, large networks will generally be very rare, but neutral correlations mean that robustness above the δ threshold is common for the biophysical GP maps. The effect can be very large. For example, for $L = 55$ RNA a recent study [43] suggests that there are about $N_P \approx 8 \times 10^{12}$ phenotypes, so that the mean frequency is $\bar{f}_p \approx 10^{-13}$. In fact all phenotype frequencies are well below the threshold $\delta = 1/(3 \times 55) = 0.00606$ above which we expect extended neutral networks. On the other hand, the mean robustness of all phenotypes was estimated to be $\bar{\rho}_p \approx 0.14 > \delta \gg \bar{f}_p$. Neutral correlations increase the probability of a nearest neighbour generating the same phenotype by about 12 orders of magnitude over the mean expectation of the null model, lifting robustness well above the threshold δ . Thus the most important way that neutral correlations contribute to evolvability is by naturally creating robustness greater than the threshold needed to generate percolating networks.

These results also pose fascinating questions relating to why or how the constraints in a GP map lead to the kinds of neutral

correlations they do. For example, we find for all three maps that the dominant relationship of robustness with frequency is $\rho_p \sim \log f_p$, a scaling that has already been pointed out earlier for RNA [13, 44]. In an interesting paper that applies concepts from network theory [36] to neutral sets, Aguirre et. al. [13] rationalise this scaling for RNA by separating out the mutational behaviour of bound and unbound bases. It would be interesting to see if a more general argument could be developed to explain the logarithmic scaling across all the systems we studied. Such analyses may help illuminate the way in which biological constraints lead to neutral correlations with their the associated robustness and large extended neutral networks.

Non-neutral mutations are important for the generation of novel variation. For all three GP maps, the probability ϕ_{qp} that a phenotype q is found by a point mutation from genotypes mapping to phenotype p is, to first order, given simply by the global frequency: $\phi_{qp} \sim f_q$, which is independent of p .

Since f_q can span many orders of magnitude, the rate at which variation appears (which scales as $\tau_q \sim 1/\phi_{qp} \sim 1/f_q$ if a population is neutrally exploring phenotype p [14]) can also range over many orders of magnitude in these systems. These large differences can lead to effects such as the *arrival of the frequent* [14], where frequent phenotypes (with larger f_q) fix in a population even when alternate phenotypes that are much more fit, but much less frequent are accessible in principle.

The reason these fitter phenotypes are not fixed is because they are unlikely to be found on evolutionary time-scales. Natural selection can only work on variation that actually arises. In the alternative case where the system is effectively in steady state, so that a less frequent phenotype has a realistic probability to arise in a population, it can still be the case, especially at larger mutation rates, that a phenotype with lower fitness but larger frequency (and robustness) will fix, an effect known as the *survival of the flattest* [45].

We should add a caveat that the absolute deviations from the simple $\phi_{qp} \sim f_q$ scaling can be fairly large, even if they are small compared to the full range on which the ϕ_{qp} vary. Also there can be biophysical effects that lead to phenotypes that are not connected at all. Nevertheless, this is usually only true for a rather small subset of all phenotypes. Finally, we note that ϕ_{qp} can be viewed as a generalisation of the phenotypic robustness, but that $\phi_{pp} = \rho_p$ scales very differently with f_p than ϕ_{qp} does when $p \neq q$. In the latter case local correlations more or less cancel out when averaged over the whole neutral set, so that $\phi_{qp} \sim f_q$, while in the former case the local correlations do not cancel out at all because robustness is fundamentally a local quantity.

It is quite striking that in all three models, a very large number of phenotypes are indeed connected to one another. The HP model merits further discussion in this regard. In a recent review [46], RNA space was compared to “a bowl of spaghetti”, because the neutral spaces were connected to most other phenotypes, while proteins were compared to a “plum pudding”, where the neutral networks were more likely to be isolated from one another. We indeed find that the neutral networks in the HP24 model are not well connected, but locate the origin of this effect in the large N_P/N_G ratio for HP24, which means that many networks are below the threshold of Eq. (7) for connections. By contrast, the compact HP5x5 model with many fewer phenotypes but a similar sized genotype space is well connected, more like “spaghetti” than like a “plum pudding”. What happens for real proteins, without the simplifying assumptions

and small system sizes typically studied in the HP model [33], remains an open question.

Another type of heterogeneity in the mapping of genotypes to phenotypes can be quantified as *local* non-neutral correlations, which occur when the local neighbourhood of genotypes are different from the global expectation given by ϕ_{qp} or f_q . We investigated two types of correlation (although one could imagine many more): i) non-neutral local over-representation correlations which result in phenotypes being more likely to be found multiple times around genotypes, and ii) non-neutral local mutational neighbourhood correlations, which mean that two genotypes connected by a neutral point mutation have mutational neighbourhoods that are more similar than do two randomly selected genotypes in a neutral set.

These two types of correlation mean that the diversity of phenotypes in the direct neighbourhood of a genotype is lower than expected from the random model or even from the averaged phenotype mutation coefficients ϕ_{qp} . Thus the rate at which a neutrally exploring population encounters novel variation will be reduced due to these correlations. How this effect influences evolvability is complex, because the term is used in many different ways in the literature [15, 47–51]. One type of evolvability simply measures the number of different phenotypes that are connected by single mutations to a neutral set [22]. While non-neutral correlations may not affect this number very much, they will affect the rate at which neutral exploration finds these new phenotypes. This lowering of the rate at which novelty appears may have a larger impact on other measures of evolvability.

Each of the three models has a deleterious phenotype which either does not fold (for RNA and the HP protein model) or does not properly assemble (in the Polyomino model for protein clusters). For all three GP maps, the folding or assembling phenotypes have fewer mutational connections to the deleterious phenotypes than would be expected by the global frequency f_{del} . This last result is perhaps the most interesting type of non-neutral correlation. It was already predicted by John Maynard Smith in his classic 1970 paper [1], where he argued that "meaningful" proteins were more likely to be neighbours of other "meaningful" proteins, and by extension, that the probability of finding a deleterious phenotype in the mutational neighbour-

hood of a "meaningful" protein would be less than by random chance. Such an effect can enhance evolutionary dynamics, because non-deleterious phenotypes are more strongly connected by mutations than expected by random chance, and so the population can more easily access potentially meaningful novel variation. Of course in practice, whether or not even the folding or self-assembling phenotypes are in fact "meaningful" will depend on the environment and other factors, but to first order a reduced propensity to mutate to manifestly deleterious phenotypes should be an advantage.

In summary, genetic correlations imply a greatly increased mutational robustness over the random expectation, which is critical to the existence of neutral networks which facilitate neutral exploration. How non-neutral correlations affect evolvability is more complex, not just because the concept itself is more diffuse, but also because the effects of correlations on evolvability are more varied.

A few final caveats are in order. In these models it is natural to use a restricted definition of a neutral mutation leading to exactly the same phenotype, whereas a more complete theory would count all mutations that are not visible to selection as effectively neutral. Thus the full picture of how these correlations affect evolutionary dynamics is complex, and depends not just on the GP map itself, but more generally on the genotype to phenotype to fitness map, for which the environment plays a key role. Moreover, population genetic parameters such as the population size and the mutation rate must be taken into account. But notwithstanding these complications, the important influence that structure in the GP map, in this case measured through the lens of genetic correlations, has on the manner in which novel variation arises (the "arrival of the fittest" [52]), and so on evolutionary dynamics, should be evident, confirming Maynard Smith's suggestions from many years ago.

ACKNOWLEDGEMENTS

The work presented here was funded by EPSRC under grant EP/P504287/1. SEA is supported by The Royal Society.

-
- [1] Smith JM. Natural selection and the concept of a protein space. *Nature*. 1970;255:563–564.
 - [2] Kimura M, et al. Evolutionary rate at the molecular level. *Nature*. 1968;217(5129):624–626.
 - [3] King J, Jukes T. Non-Darwinian evolution. *Science (New York, NY)*. 1969;164(881):788.
 - [4] Lipman DJ, Wilbur WJ. Modelling neutral and selective evolution of protein folding. *Proceedings of the Royal Society of London Series B: Biological Sciences*. 1991;245(1312):7–11.
 - [5] Dill KA. Theory for the folding and stability of globular proteins. *Biochemistry*. 1985;24(6):1501–1509.
 - [6] Lau KF, Dill KA. A lattice statistical mechanics model of the conformational and sequence spaces of proteins. *Macromolecules*. 1989;22(10):3986–3997.
 - [7] Schuster P, Fontana W, Stadler PF, Hofacker IL. From sequences to shapes and back: A case study in RNA secondary structures. *Proceedings: Biological Sciences*. 1994;255(1344):279–284.
 - [8] Hofacker IL, Fontana W, Stadler PF, Bonhoeffer LS, Tacker M, Schuster P. Fast folding and comparison of RNA secondary structures. *Monatshefte für Chemie/Chemical Monthly*. 1994;125(2):167–188.
 - [9] Mathews DH, Disney MD, Childs JL, Schroeder SJ, Zuker M, Turner DH. Incorporating chemical modification constraints into a dynamic programming algorithm for prediction of RNA secondary structure. *Proceedings of the National Academy of Sciences of the United States of America*. 2004;101(19):7287–7292.
 - [10] Reuter JS, Mathews DH. RNAstructure: software for RNA secondary structure prediction and analysis. *BMC bioinformatics*. 2010;11(1):129.
 - [11] Fontana W. Modelling 'evo-devo' with RNA. *BioEssays*. 2002;24(12):1164–1177.
 - [12] Cowperthwaite MC, Economo EP, Harcombe WR, Miller EL, Meyers LA. The ascent of the abundant: how mutational networks constrain evolution. *PLoS computational biology*. 2008;4(7):e1000110.
 - [13] Aguirre J, Buldú JM, Stich M, Manrubia SC. Topological structure of the space of phenotypes: the case of RNA neutral networks. *PloS one*. 2011;6(10):e26324.
 - [14] Schaper S, Louis AA. The Arrival of the Frequent: How Bias in Genotype-Phenotype Maps Can Steer Populations to Local Optima. *PloS one*. 2014;9(2):e86635.

- [15] Wagner A. Robustness and evolvability in living systems. Princeton University Press Princeton, NJ.; 2005.
- [16] Wagner A. The Origins of Evolutionary Innovations: A Theory of Transformative Change in Living Systems. Oxford University Press; 2011.
- [17] Ciliberti S, Martin OC, Wagner A. Robustness can evolve gradually in complex regulatory gene networks with varying topology. *PLoS computational biology*. 2007;3(2):e15.
- [18] Raman K, Wagner A. Evolvability and robustness in a complex signalling circuit. *Mol BioSyst*. 2011;.
- [19] Samal A, Rodrigues JFM, Jost J, Martin OC, Wagner A. Genotype networks in metabolic reaction spaces. *BMC systems biology*. 2010;4(1):30.
- [20] Greenbury SF, Johnston IG, Louis AA, Ahnert SE. A tractable genotype–phenotype map modelling the self-assembly of protein quaternary structure. *Journal of The Royal Society Interface*. 2014;11(95):20140249.
- [21] Ohta T. Slightly deleterious mutant substitutions in evolution. *Nature*. 1973;246(5428):96–98.
- [22] Wagner A. Robustness and evolvability: a paradox resolved. *Proceedings of the Royal Society B*. 2008;275(1630):91.
- [23] Wright SG. The roles of mutation, inbreeding, crossbreeding and selection in evolution. *Proc 6th Int Cong Genet*. 1932;1:356–366.
- [24] Schultes EA, Bartel DP. One sequence, two ribozymes: implications for the emergence of new ribozyme folds. *Science*. 2000;289(5478):448–452.
- [25] Hayden EJ, Ferrada E, Wagner A. Cryptic genetic variation promotes rapid evolutionary adaptation in an RNA enzyme. *Nature*. 2011;474(7349):92–95.
- [26] Payne JL, Wagner A. The Robustness and Evolvability of Transcription Factor Binding Sites. *Science*. 2014;343(6173):875–877.
- [27] Ferrada E, Wagner A. A comparison of genotype-phenotype maps for RNA and proteins. *Biophysical journal*. 2012;102(8):1916–1925.
- [28] Wagner A. The molecular origins of evolutionary innovations. *Trends in Genetics*. 2011;27(10):397–410.
- [29] Ahnert S, Johnston I, Fink T, Doye J, Louis A. Self-assembly, modularity, and physical complexity. *Physical Review E*. 2010;82(2):026117.
- [30] Johnston IG, Ahnert SA, Doye JPK, Louis AA. Evolutionary Dynamics in a Simple Model of Self-Assembly. *Physical Review E*. 2011;83:066105.
- [31] Irbäck A, Troein C. Enumerating designing sequences in the HP model. *Journal of Biological Physics*. 2002;28(1):1–15.
- [32] Li H, Helling R, Tang C, Wingreen N. Emergence of preferred structures in a simple model of protein folding. *Science*. 1996;273(5275):666.
- [33] Schram RD, Schiessel H. Exact enumeration of Hamiltonian walks on the $4 \times 4 \times 4$ cube and applications to protein folding. *Journal of Physics A: Mathematical and Theoretical*. 2013;46(48):485001.
- [34] Reidys C, Stadler PF, Schuster P. Generic properties of combinatorial maps: neutral networks of RNA secondary structures. *Bulletin of mathematical biology*. 1997;59(2):339–397.
- [35] Schaper S, Johnston IG, Louis AA. Epistasis can lead to fragmented neutral spaces and contingency in evolution. *Proceedings of the Royal Society B: Biological Sciences*. 2011;p. rspb20112183.
- [36] Newman M. Networks: an introduction. Oxford University Press; 2010.
- [37] Sumedha, Martin OC, Peliti L. Population size effects in evolutionary dynamics on neutral networks and toy landscapes. *J Stat Mech: Theory and Experiment*. 2007;2007(05):P05011.
- [38] Bhattacharyya A. On a Measure of Divergence between Two Multinomial Populations. *Sankhyā: The Indian Journal of Statistics (1933-1960)*. 1946;7(4):pp. 401–406.
- [39] Conrad M. Natural selection and the evolution of neutralism. *BioSystems*. 1982;15(1):83–85.
- [40] Van Nimwegen E, Crutchfield JP, Huynen M. Neutral evolution of mutational robustness. *Proceedings of the National Academy of Sciences*. 1999;96(17):9716–9720.
- [41] Masel J, Siegal ML. Robustness: mechanisms and consequences. *Trends in Genetics*. 2009;25(9):395–403.
- [42] Draghi JA, Parsons TL, Wagner GP, Plotkin JB. Mutational robustness can facilitate adaptation. *Nature*. 2010;463(7279):353–355.
- [43] Dingle K, Schaper S, Louis AA. The structure of the genotype-phenotype map strongly constrains the evolution of non-coding RNA. *arxiv*. 2015;.
- [44] Jorg T, Martin OC, Wagner A. Neutral network sizes of biological RNA molecules can be computed and are not atypically small. *BMC bioinformatics*. 2008;9(1):464.
- [45] Wilke CO, Wang J, Ofria C, Lenski RE, Adami C. Digital organisms: survival of the flattest. *Nature*. 2001;412:331–333.
- [46] Goldstein RA. The structure of protein evolution and the evolution of protein structure. *Current opinion in structural biology*. 2008;18(2):170–177.
- [47] Conrad M. The geometry of evolution. *BioSystems*. 1990;24(1):61–81.
- [48] Wagner GP, Altenberg L. Perspective: complex adaptations and the evolution of evolvability. *Evolution*. 1996;p. 967–976.
- [49] Kirschner M, Gerhart J. Evolvability. *Proc Natl Acad Sci USA*. 1998 July;95(15):8420–8427.
- [50] Dawkins R. The Evolution of Evolvability. *Artificial Life*. 1989;p. 201–220.
- [51] Pigliucci M. Is evolvability evolvable? *Nature Reviews Genetics*. 2008;9(1):75–82.
- [52] Wagner A. Arrival of the Fittest: Solving Evolution’s Greatest Puzzle. Penguin; 2014.
- [53] Schuster P, Fontana W, Stadler PF, Hofacker IL. From Sequences to Shapes and Back: A Case Study in RNA Secondary Structures. *Proceedings of the Royal Society of London B: Biological Sciences*. 1994;255(1344):279–284.

Appendix A: An extended analysis of ϕ_{qp}

In this section, we consider a more detailed analysis of the relationship between ϕ_{qp} and f_p . We focus in particular on the theoretical threshold proposed in Eq. (7) and in a variety of phenotypes in the smaller RNA12, $S_{2,8}$ and HP24 GP maps.

1. Associated analytical results of the sampling threshold

We begin with an analysis of the sampling threshold γ from average phenotypes in a given GP map. We showed that for effective sampling, we require

$$f_q > \frac{1}{F_p(K-1)L}$$

which may be expressed alternatively as

$$f_p f_q > \frac{1}{K^L(K-1)L}$$

The average phenotype frequency may be written down as

$$\langle f \rangle_{\text{phenotype}} = \frac{1}{N_P} \sum_i f_i = \frac{1}{N_P}$$

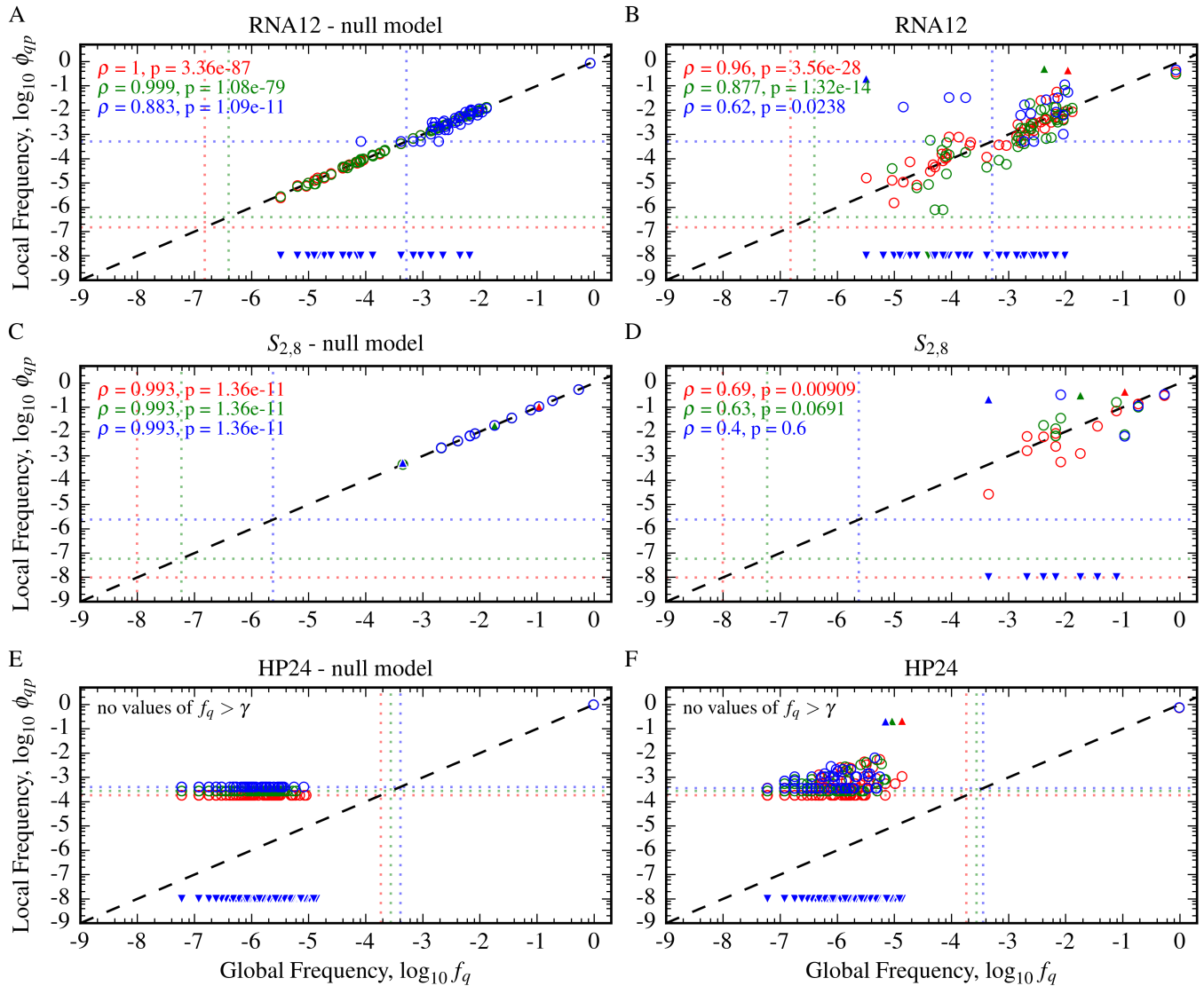


FIG. 9. **The relationship between ϕ_{qp} and f_q is more complex in smaller GP maps.** Local frequency of phenotypes q around genotypes with phenotype p (ϕ_{qp}) are plotted against the frequency of phenotypes q (f_q) for each biological GP map and a random null model counterpart. The black dashed line is $\phi_{qp} = f_q$. The dotted lines are $\phi_{qp} = \gamma$ and $f_q = \gamma$ (c.f. Eq. (7)). In each case, three different phenotypes p with different frequencies in the GP map are considered (represented with red, green and blue from largest to smallest f_p). (A, C and E) We plot local against global frequency for the random null models. $S_{2,8}$ and HP24 illustrate the two regimes where $f_q > \gamma$ and $f_q < \gamma$ in all cases respectively. The former has local frequencies strongly determined by global frequency ($\phi_{qp} = f_q$), while in the latter, occurrences of phenotypes are rare; they may not occur at all (downward triangular points, $\phi_{qp} = 0$) or they simply occur a single time ($\phi_{qp} = \gamma$). In the RNA12 null model, we see the blue phenotype crossing the threshold with some phenotypes having $f_q \approx \gamma$. (B, D, F) The three phenotypes are considered in each biological GP map. For larger frequency phenotypes (red and green in RNA12 and $S_{2,8}$), we find that local frequency is, to first order, well determined by the global frequency in line with the random null models (up to an order of magnitude variation in local frequency in comparison to global frequency). For lower frequency phenotypes (blue in RNA12 and $S_{2,8}$), we see that phenotype correlations are more important, an intuitive result given the genotypes of p will be less encompassing of the whole GP map in these cases. In HP24 all frequencies are well below the gamma threshold but we still see a positive (although weaker) relationship between local frequency and global frequency (unlike in the null model, where ϕ_{qp} remains flat with respect to f_q for $f_q < \gamma$). This is due to the presence of neutral correlations, an effect discussed in greater detail in the main text.

or with respect to the genotype sampling distribution as

$$\langle f \rangle_{\text{genotype}} = \sum_i f_i^2$$

Substituting in the smaller of the two, the average phenotype frequency, and then considering the required threshold for effectively sampling phenotype q from the average phenotype p ,

we find

$$f_q > \frac{N_P}{K^L(K-1)L}$$

For RNA, where empirical scaling values are known ($N_P \approx 1.5 \times L^{-\frac{3}{2}} 1.8^L$ [53]), we can further write

$$f_q \gtrsim 0.45^L \frac{1}{L^{\frac{5}{2}}}$$

for a phenotype q to be effectively sampled.

We can change the question of effective sampling to ask the conditions on N_P for the average phenotype q to be accessed from the average phenotype p . In these circumstances, we can see that

$$N_P < \sqrt{K^L(K-1)L}$$

which RNA satisfies to an increasing extent for increasing L , as N_p scales with 1.8^L while the right-hand side scales with 2^L .

Finally, we can also write down the approximate fraction less than the average phenotype frequency that is accessible from an average phenotype, through expressing $f_q = \chi \langle f \rangle_{\text{phenotype}}$, which leads to a threshold fraction

$$\chi = \frac{N_P^2}{K^L(K-1)L}$$

Again, using RNA as an example system this leads to

$$\chi \propto 0.81^L \frac{1}{L^4}$$

for a given length of RNA, showing that an increasing fraction of phenotypes with frequencies below the average may be effectively sampled from the average phenotype.

2. Extended analysis of ϕ_{qp}

In this section, in contrast to the analysis in the main body considering the frequency of phenotypes q around phenotype p where $f_p \ll \gamma$, we consider different p across a range of phenotype frequencies f_p in the GP map. In the random null model, at values of $f_q > \gamma$, we expect phenotypes to almost exactly follow $\phi_{qp} = f_q$. When $f_q < \gamma$, there are two likely possibilities for a given phenotype: either the phenotype is not found at all ($\phi_{qp} = 0$) or it is found a single time ($\phi_{qp} = \gamma$). The latter is an over-representation of the local prevalence of q for the GP map, while the former is clearly no local representation at all.

In Fig. 9, we display three pairs of plots for the RNA12, $S_{2,8}$ and HP24 GP maps and a randomised null model counterpart. The null models are displayed on the left, with the actual GP maps on the right. In each plot, we show the values of ϕ_{qp} against f_q for three different phenotypes p (coloured by data point as red, blue and green, with red the largest frequency phenotype and blue the smallest). Upward triangular data points represent values for ϕ_{pp} , downward triangular

data points $\phi_{qp} = 0$ (shown at $1e-8$ for visualisation purposes only) and the circular data points are all other phenotypes. Vertical and horizontal dotted coloured lines represent $f_q = \gamma$ and $\phi_{qp} = \gamma$ respectively. The diagonal dashed black line is $\phi_{qp} = f_q$, the null expectation for phenotypes with $f_q > \gamma$.

We begin by discussing the behaviour of the null model. The $S_{2,8}$ and HP24 null models provide the extreme cases. For $S_{2,8}$, all phenotypes are highly frequent and have $f_q \gg \gamma$. Consequently, we see that each of the three phenotypes follows the expected trend of $\phi_{qp} = f_q$ to a very high degree of accuracy (Spearman rank correlation coefficient and p-value in the top left). For the HP24 null model, all frequencies are such that $f_q \ll \gamma$. As such, phenotypes that are found locally are found only once ($\phi_{qp} = \gamma$) and most are not found at all (the many downward triangular points). For the RNA12 null model, the frequency of phenotypes used for phenotype p span the range of all $f_q \gg \gamma$ (red and green) and to some phenotypes having $f_q \approx \gamma$ (blue). As a result, we see the red and green phenotypes follow $\phi_{qp} = f_q$ strongly, while the tail of the blue phenotype has fluctuations between the three behaviours.

The results from the null models demonstrate the accuracy of the above outlined intuition for a null relationship between the local connectivities of phenotypes with respect to the global abundance. With this in mind, we can now draw direct comparisons between each phenotype in the null model and actual behaviour exhibited in the biological GP maps. For each of the GP maps, we plot the same phenotype as in the null model case. For RNA12, positive correlations are found for each phenotype, with deviations from $\phi_{qp} = f_q$ being more pronounced for lower frequency phenotypes (blue is subject to much greater fluctuations than red). The fluctuations are approximately up to an order of magnitude either side of the $\phi_{qp} = f_q$. We see a similar behaviour for $S_{2,8}$, with the largest fluctuations exhibited for the low frequency blue phenotype.

Finally, we consider the biological HP24 GP map. As was the case in the null model version, every phenotype (apart from the deleterious phenotype) lies in the region where $f_q \ll \gamma$. The notable difference in the actual GP map is the tendency for phenotypes with a larger f_q to also be more likely to be locally present ($\log \phi_{qp} \propto \log f_q$). We can understand this with the following rationale: due to the neutral correlations present, if a single genotype with phenotype q is found locally, then it is also likely that other genotypes with phenotype q will be local to genotypes with phenotype p . And due to this effect being more pronounced for phenotypes with a greater frequency ($\rho_p \propto \log f_p$, c.f. Fig. 2), we also see this effect locally with increased f_q resulting in a greater ϕ_{qp} , leading to the positive proportionality between $\log \phi_{qp}$ and $\log f_q$ in the actual GP maps when compared to the null models.